REFERENCES

[1] A. J. Ptak, S. Kurtz, C. Curtis, R. Reedy and J. M. Olson. Incorporation effects in MOCVD-grown (In)GaAsN using different nitrogen precursors. *J. Crystal Growth* **243** (2002): 231-237.

[2] G. Mussler, L. Daweritz and K. H. Ploog. Thickness dependent roughening of Ga(As,N)/GaAs MQW structures with high nitrogen content. *J. Crystal Growth* **251** (2003): 399-402.

[3] M. Weyers, M. Sato and H. Ando. Growth of GaAsN alloys by low-pressure metalorganic chemical vapor deposition using plasma-cracked NH_3. *Appl. Phys. Lett.* **62** (1993): 1396-1398.

[4] W. G. Bi and C. W. Tu. Bowing parameter of the bandgap energy of GaN_xAs_{1-x}. *Appl. Phys. Lett.* **70** (1997): 1608-1610.

[5] I. A. Buyanova, W. M. Chen and B. Monemar. Electronic properties of Ga(In)NAs alloys. *MRS Internet J. Nitride Semicond. Res.* **6** (2001): 1-16.

[6] K. Uesugi and I. Suemune. Bandgap energy of GaNAs alloys grown on (001) GaAs by metalorganic molecular beam epitaxy. *Jpn. J. Appl. Phys.* **36** (1997): L1572-L1575.

[7] S. Sakai, Y. Ueta and Y. Terauchi. Band gap energy and band lineup of III-V alloy semiconductors incorporating nitrogen and boron. *Jpn. J. Appl. Phys.* **32** (1993): 4413-4417.

[8] M. Kondow, K. Uomi, A. Niwa, T. Kitatani, S. Watahiki and Y. Yazawa. GaInNAs: A novel material for long-wavelength-range laser diodes with excellent high-temperature performance. *Jpn. J. Appl. Phys.* **35** (1996): 1273-1275.

[9] C. W. Tu and P. K. L. Yu, Material properties of III-V semiconductors for lasers and detectors. *MRS bulletin* May (2003): 345-349.

[10] J. Toivonen, T. Hakkarainen, M. Sopanen and H. Lipsanen. High nitrogen composition GaAsN by atmospheric pressure metalorganic vapor-phase epitaxy. *J. Crystal Growth* **221** (2000): 456-460.

[11] L. H. Li, Z. Pan, W. Zhang, Y. W. Lin, Z. Q. Zhou and R. H. Wu. Effects of rapid thermal annealing on the optical properties of GaN_xAs_{1-x}/GaAs

single quantum well structure grown by molecular beam epitaxy. *J. Appl. Phys.* **87** (2000): 245-248.

[12] C. T. Foxon, T. S. Cheng, S. V. Novikov, D. E. Lacklison, L. C. Jenkins, D. Johnston, J. W. Orton, S. E. Hooper, N. Baba-Ali, T. L. Tansley and V. V. Tretyakov. The growth and properties of group III nitrides. *J. Crystal Growth* **150** (1995): 892-896.

[13] Z. L. Liu, P. P. Chen, T. X. Li, C. J. Xu, W. Lu, F. Z. Wang, Z. H. Chen. Effect of rapid thermal annealing on the optical properties of MBE growth GaNAs films. *J. Luminescence* **119-120** (2006): 546-550.

[14] F. Nakajima, S. Sanorpim, W. Ono, R. Katayama and K. Onabe. MOVPE growth and optical characterization of GaAsN films with higher nitrogen concentrations. *phys. stat. sol. (a)* **203** (2006): 1641-1644.

[15] H. Dumont, L. Auvray, Y. Monteil. F. Saidi, F. Hassen, H. Maaref. Radiative N-localized recombination and confinement in GaAsN/GaAs epilayers and quantum well structures. *Optical materials* **24** (2003): 303-308.

[16] S. Z. Wang, S. F. Yoon, W. K. Loke, C. Y. Liu and S. Yuan. Origin of photoluminescence of GaAsN/GaN(001) layers grown by plasma-assisted solid source molecular beam epitaxy. *J. Crystal Growth* **255** (2003): 258-265.

[17] W. J. Fan, S. F. Yoon, W. K. Cheah, W. K. Loke, T. K. Ng, S. Z. Wang, R. Liu and A. Wee. Determination of nitrogen composition in $GaAs_{1-x}N_x$ epilayer on GaAs. *J. Crystal Growth* **268** (2004): 470-474.

[18] S.-H. Wei and A. Zunger. Calculated natural band offsets of all II–VI and III–V semiconductors: Chemical trends and the role of cation *d* orbitals. *Appl. Phys. Lett.* **72** (1998): 2011-2013.

[19] I. Akasaki and H. Amano. Crystal growth and conductivity control of group III nitride semiconductors and their application to short wavelength light emitters. *Jpn. J. Appl. Phys.* **36** (1997): 5393-5408.

[20] G. Vincent, D. Bois and A. Chantre. Photoelectric memory effect in GaAs. *J. Appl. Phys.* **53** (1982): 3643-3649.

[21] S. M. Sze. *Physics of Semiconductor Devices.* John Wiley & Sons, New York, 1981.

[22] K. Kim, W. R. L. Lambrecht, B. Segall and M. van Schilfgaarde. Effective masses and valence-band splitting in GaN and AlN. *Phys. Rev. B* **56** (1997): 7363-7375.

[23] T. B. Bateman, H. J. McSkimin, and J. M. Whelan. Elastic moduli of single-crystal gallium arsenide. *J. Appl. Phys.* **30** (1959): 544-545.

[24] M. Takahashi, A. Moto, S. Tanaka, T. Tanabe, S. Takagishi, K. Karatani, M. Nakayama, K. Matsuda and T. Saiki. Observation of compositional fluctuations in GaNAs alloys grown by metalorganic vapor-phase epitaxy. *J. Crystal Growth* **221** (2000): 461-466.

[25] R. Bhat, C. Caneau, L. Salamanca-Riba, W. Bi, and C. Tu. Growth of GaAsN/GaAs, GaInAsN/GaAs and GaInAsN/GaAs quantum wells by low-pressure organometallic chemical vapor deposition. *J. Crystal Growth* **195** (1998): 427-437.

[26] U. Tisch, E. Finkman and J. Salzman. The anomalous bandgap bowing in GaAsN. *Appl. Phys. Lett.* **81** (2002): 463-465.

[27] W. Shan, W. Walukiewicz, J. W. Ager III, E. E. Haller, J. F. Geisz, D. J. Friedman, J. M. Olson and S. R. Kurtz. Band anticrossing in GaInNAs. *Phys. Rev. Lett.* **82** (1999): 1221-122.

[28] J. Wu, W. Shan and W. Walukiwicz. Band anticrossing in highly mismatched III–V semiconductor alloys. *Semicond. Sci. Technol.* **17** (2002): 860-869.

[29] W. Walukiewicz. Narrow band gap group III-nitride alloys. *Physica E* **20** (2004): 300-307.

[30] E. P. OReilly. Valence band engineering in strained-layer structures. *Semicond. Sci. Technol.* **4** (1989): 121-137.

[31] J. Singh. *Physics of semiconductor and Their Heterostructure*. Singapore: McGraw-Hill, 1993.

[32] J. H. Davies. *The Physics of Low-Dimensionol Semiconductors: An Introduction*, Cambridge University Press, 1999.

[33] R. Songmuang. *Study of optically pumped edge emission spectra from quantum structure.* Master's thesis, Department of Electrical Engineering, Faculty of Engineering, Chulalongkorn University, Thailand, 1999.

[34] W. T. Masselink, P. J. Pearah, C. K. Peng, H. Morkoo, G. D. Sanders and Yia-Chung Chang. Absorption coefficients and exciton oscillator strengths in AlGaAs-GaAs super lattices. *Phys. Rev B* **32** (1985): 8027-8034.

[35] M. Balkanski and R. F. Wallis. *Semiconductor Physics and Applications.* Oxford University press, 2000.

[36] S. Sakai and T. Abe, Band lineup of nitride-alloy heterostructures, *in 41st Spring Meet. Jpn. Soc. Appl. Phys., Tokyo, Japan* (1994): 186.

[37] C. S. Park, T. S. Kim, J. Y. Park, T. V. Cuong, H. W. Shim, E.-K. Suh and C. H. Hong. The influence of well and barrier conditions on InGaAsN/GaAs multiple quantum wells grown by using MOCVD. *J. the Korean Physical Society* **43** (2003): 1096-1100.

[38] K. Uesugi, N. Morooka and I. Suemune. Reexamination of N composition dependence of coherently grown GaNAs band gap energy with high-resolution X-ray diffraction mapping measurements. *Appl. Phys. Lett.* **74** (1999): 1254-256.

[39] M. J. Seong, M. C. Hanna and A. Mascarenhas. Composition dependence of Raman intensity of the nitrogen localized vibrational mode in $GaAs_{1-x}N_x$. *Appl. Phys. Lett.* **79** (24) (2001): 3974-3976.

[40] L. Grenouillet, C. Bru-Chevallier G. Guillot, P. Ballet, P. Duvaut, G. Rolland, and A. Million. Rapid thermal annealing in GaN_xAs_{1-x}/GaAs structures: Effect of nitrogen reorganization on optical properties. *J. Appl. Phys.* **91** (2002): 5902-5908.

[41] Fang-I. Lai, S. Y. Kuo, J. S. Wang, R. S. Hsiao, H. C. Kuo, J. Chi, S. C. Wang, H. S. Wang, C. T. Liang, Y. F. Chen. Temperature-dependent optical properties of $In_{0.34}Ga_{0.66}As_{1-x}N_x$/GaAs single quantum well with high nitrogen content for 1.55 μm application grown by molecular beam epitaxy. *J. Crystal Growth* **291** (2006): 27-33.

[42] M.-A. Pinault and E. Tournie. On the origin of carrier localization in $Ga_{1-x}In_xN_yAs_{1-y}$/GaAs quantum wells. *Appl. Phys. Lett.* **78** (2001): 1562-1564.

[43] I. Vurgaftman, J. R. Meyer and L. R. Ram-Mohan. Band parameters for III–V compound semiconductors and their alloys. *J. Appl. Phys.* **89** (2001): 5815-5875.

[44] M. Kozhevnikov, V. Narayanamurti, C. V. Reddy, H. P. Xin, C. W. Tu, A. Mascarenhas and Y. Zhang. Evolution of $GaAs_{1-x}N_x$ conduction states and giant Au/$GaAs_{1-x}N_x$ Schottky barrier reduction studied by ballistic electron emission spectroscopy. *Phys. Rev. B* **61** (2000): R7861-R7864.

APPENDICES

APPENDIX A

INTERNATIONAL SCIENTIFIC PAPER

Available online at www.sciencedirect.com
ScienceDirect
Journal of Crystal Growth 298 (2007) 140–144
JOURNAL OF CRYSTAL GROWTH
www.elsevier.com/locate/jcrysgro

Post-growth thermal annealing of high N-content GaAsN by MOVPE and its effect on strain relaxation

Pawinee Klangtakai[a], Sakuntam Sanorpim[a,*], Kajornyod Yoodee[a], Wataru Ono[b], Fumio Nakajima[b], Ryuji Katayama[b], Kentaro Onabe[b]

[a]*Department of Physics, Faculty of Science, Chulalongkorn University, Phayathai Rd., Pathumwan, Bangkok 10330, Thailand*
[b]*Department of Advanced Materials Science, University of Tokyo, 5-1-5 Kashiwanoha, Kashiwa, Chiba 277-8561, Japan*

Available online 4 December 2006

Abstract

We report on the further investigation of the effect of post-growth thermal annealing on optical and structural properties of the high N-content $GaAs_{0.949}N_{0.051}$ layer grown on a GaAs(0 0 1) substrate by metalorganic vapor phase epitaxy (MOVPE). Photoluminescence (PL) spectroscopy was performed to measure the energy positions of the near band edge excitonic emission. The high-resolution X-ray diffraction and Raman spectroscopy were conducted to examine the lattice parameters, also the N concentration of the layers annealed at 650 °C with different annealing times. The layer subjected to thermal anneals exhibits an increasing of N incorporation, a strain relaxation and a blue shift of the PL peak energy. For such high N-containing layer, the interstitial N atoms generated in the growth process may replace the As atoms/vacancies on the lattice sites to become more stable substitutional N atoms through the thermal annealing process, which will produce the strain relaxation, in addition to an improvement of the alloy uniformity. Our results suggest the two major effects: (i) the reorganization of N and (ii) the strain relaxation in the GaAsN layer that can be explained the blue shift in the PL peak energy after annealing.

PACS: 61.10.Nz; 68.37.Yz; 78.30.Fs; 78.55.Cr; 78.66.Fd; 81.11.Kk

Keywords: A1. High-resolution X-ray diffraction; A1. Optical property; A3. Metalorganic vapor phase epitaxy; B2. III–V-nitrides; B3. Laser diodes

1. Introduction

Great efforts have recently been devoted to the preparation of high-quality GaAsN films with high N incorporation, the characterization of GaAsN films, the development of devices using GaAsN-based materials. Low-bandgap Ga(In)AsN-based heterostructures are expected as useful for optoelectronic devices such as laser diodes emitting at 1.3 and 1.55 μm for optical communication systems [1–3]. The GaAsN films with N contents up to 5–8% were grown on a GaAs(0 0 1) substrate by metalorganic vapor phase epitaxy (MOVPE) [4–6]. However, the optical quality of GaAsN has been found to degrade with higher N incorporation. This may be due to comparatively to the lower growth temperature commonly used for the III–V nitrides, compared to that for GaAs. Post-growth thermal annealing can improve the luminescence properties significantly, but leads to a blue shift of the photoluminescence (PL) peak energy [7–9]. The structural origin of the effects of post-growth annealing treatments has been an issue. However, there are presently few reports on the effect of post-growth thermal annealing on the high N-containing GaAsN films [4,10,11].

Previously, we reported the results on the MOVPE growth of the high N-content GaAsN films with N content range of 0–5.1% using 1,1-dimethylhydrazine (DMHy), and tertiarybutylarsine (TBAs) as the source materials for N and As, respectively [11]. In this work, we have investigated the influence of the post-growth thermal annealing on structural and optical properties of the high N-content $GaAs_{0.949}N_{0.051}$ film.

*Corresponding author. Tel.: +66 (0)2 218 5110; fax: +66 (0)2 253 1150.
E-mail address: Sakuntam.S@chula.ac.th (S. Sanorpim).

0022-0248/$ - see front matter © 2006 Elsevier B.V. All rights reserved.
doi:10.1016/j.jcrysgro.2006.10.111

2. Experiments

The GaAsN layer with N content of 5.1% was grown on a GaAs(0 0 1) substrate at 500 °C by MOVPE using trimethylgallium (TMGa), DMHy, and TBAs as the source materials for Ga, N, and As, respectively. The thickness of the GaAsN layer was examined by high-resolution X-ray diffraction (HRXRD) to be about 200 nm. The N content in an as-grown layer was determined from a symmetrical (0 0 4) and an asymmetrical (1 1 5) reflections using HRXRD [6,7], by assuming a linear dependence of lattice constant (a_0) on the N content [12].

The post-growth thermal annealing was performed in the growth reactor under TBAs environment at 650 °C for 2 and 5 min. To investigate the influences of the annealing on structural and optical qualities, HRXRD, PL, and Raman scattering measurements were performed. In order to evaluate the strain relaxation precisely, reciprocal lattice mapping of asymmetrical (1 1 5) reflection was carried out for all annealed samples.

3. Results and discussion

To evaluate the N concentration in the GaAsN grown layer on a GaAs(0 0 1) substrate, it is required to know the lattice parameters of the epilayer perpendicular ($a_\perp$) and parallel ($a_\parallel$) to the GaAs(0 0 1) surface, which are generally calculated from a symmetric (0 0 4) and an asymmetric (1 1 5) HRXRD, respectively. Fig. 1a shows a (0 0 4) HRXRD $2\theta/\omega$ scan of the GaAsN layer on GaAs(0 0 1) substrate. From the separation between the GaAs and GaAsN reflection peaks, the $a_\perp$ was determined to be 5.544 Å. In addition, Pendellösung fringes are clearly visible due to a finite thickness and high structural quality of the grown layer. It is also shown that the spacing between the nearest fringes corresponds to a layer thickness of 200 nm. Fig. 1b shows a reciprocal space map of the (1 1 5) reflection. It is clearly seen that the GaAsN layer is coherently strained and exhibits a good epitaxial quality. By using both the (0 0 4) $2\theta/\omega$ scan and the (1 1 5) reciprocal space mapping measurements [7], the in-plane lattice parameter, $a_\parallel$, was determined to be 5.653 Å. Note that this value is in an excellent agreement with the lattice constant of GaAs. Thus, the N concentration, which can be estimated from the lattice parameters using Vegard's law [7], was determined to be 5.1%. HRXRD results demonstrate that a high epitaxial quality and coherently strained GaAsN layer with N content as high as 5.1% was successfully grown. However, it is found that the lumines-

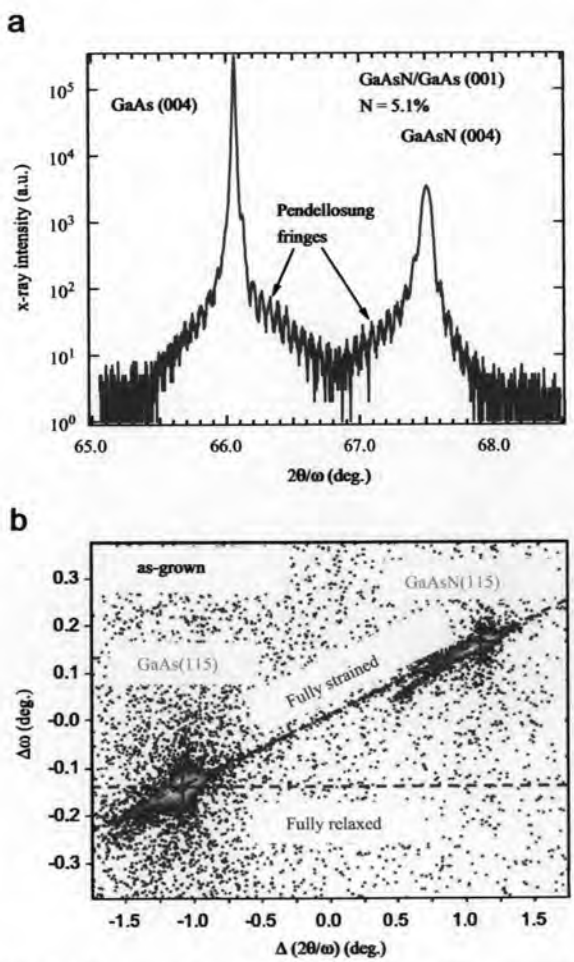

Fig. 1. (a) Symmetrical (0 0 4) HRXRD $2\theta/\omega$ curve and (b) asymmetric (1 1 5) reciprocal lattice map of the as-grown $GaAs_{0.949}N_{0.051}$ layer.

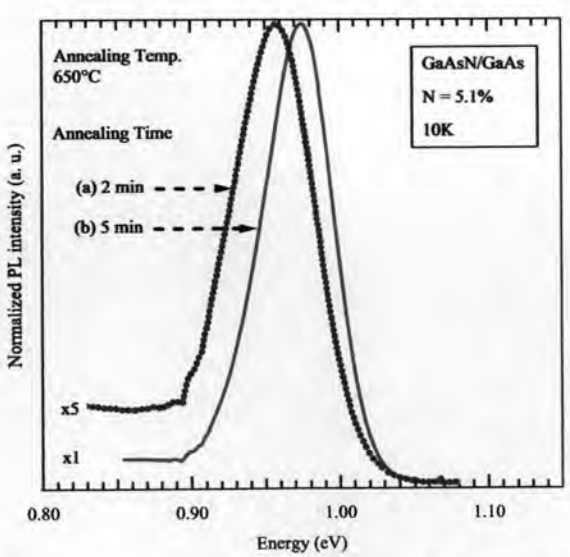

Fig. 2. Low-temperature (10 K) PL spectra of the annealed $GaAs_{0.949}N_{0.051}$ layers at 650 °C for different annealing times: (a) 2 min and (b) 5 min.

cence signal cannot be detected from this GaAsN layer. This is due to a highly nonradiative recombination centers in such high N-containing samples.

Fig. 2 illustrates low-temperature (10 K) PL spectra of the $GaAs_{0.949}N_{0.051}$ layer annealed at 650 °C for annealing times of (a) 2 min and (b) 5 min. After annealing, the changes in the PL peak energy, the values of a full-width at half-maximum (FWHM) and the PL-integrated intensity were clearly observed. Each PL spectrum is a single peak without any deep-level-related luminescence and low-energy tail. The temperature-dependent PL of the peak energy of the annealed layers was also investigated [11]. With increasing temperature, a red-blue-red shift of the PL peak position was clearly observed. At low temperatures, it is found that the PL emission is mainly related to the recombination at the localized states, while at high temperatures, band edge emissions are the primary origin. As a result, it is important to note that the PL spectra exhibit the characteristics of a near band edge excitonic emission [11,13]. This emission showed a substantial blue shift with the longer annealing time, and the long wavelength emission at about 1.3 μm (0.95 eV) was recorded at 10 K. In general meaning, the blue shift has been attributed mainly to the following possible reasons:

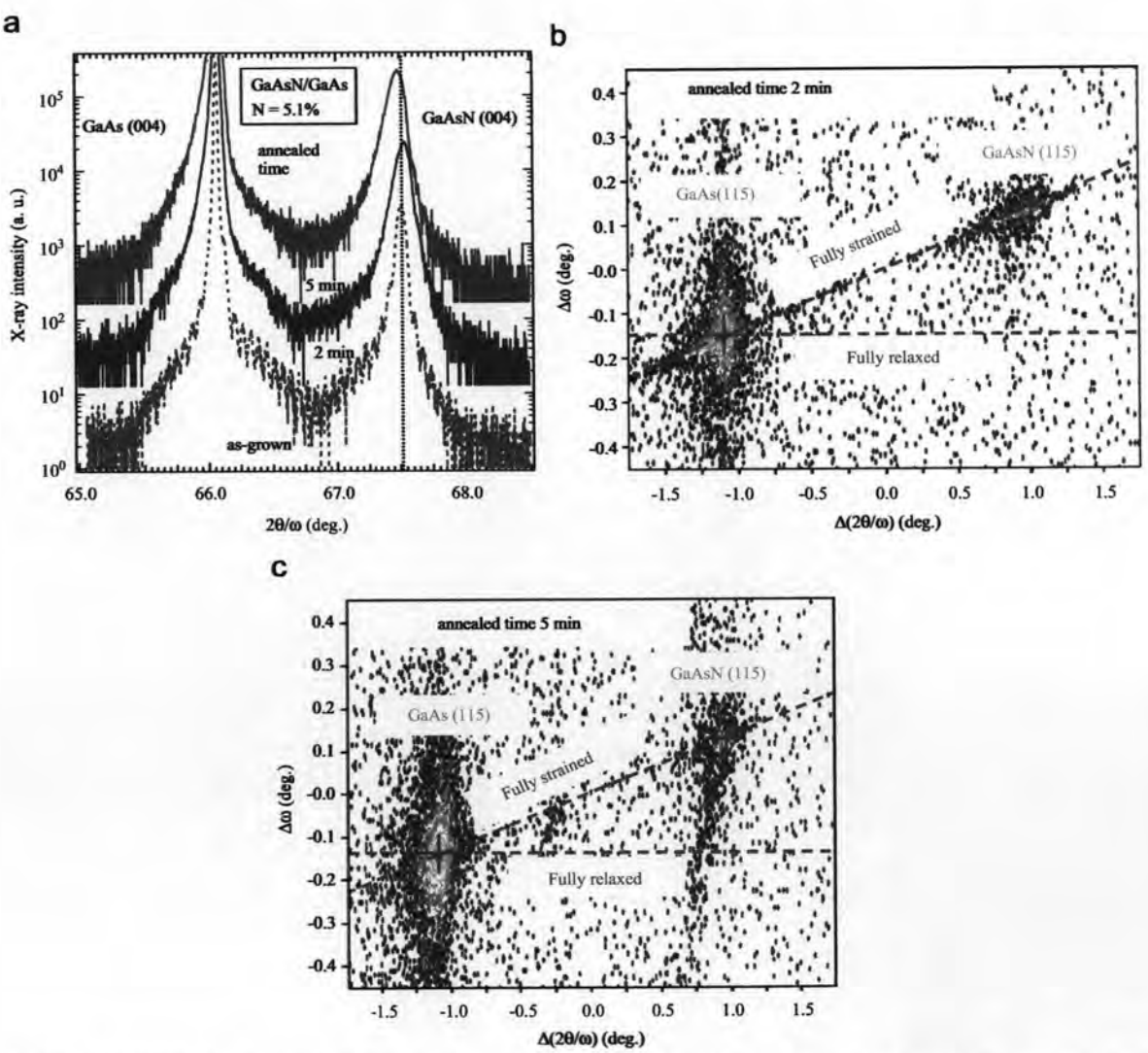

Fig. 3. (a) (0 0 4) HRXRD $2\theta/\omega$ curves of the as-grown and annealed (650 °C for 2 and 5 min) $GaAs_{0.949}N_{0.051}$ layer. Reciprocal lattice maps of the (1 1 5) reflection of the $GaAs_{0.949}N_{0.051}$ layers annealed at 650 °C for (b) 2 min and (c) 5 min.

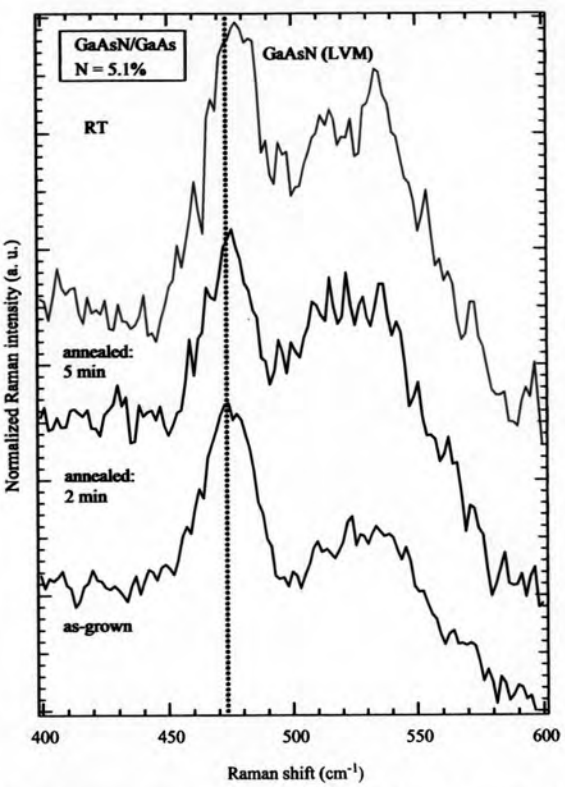

Fig. 4. Raman spectra of the as-grown and annealed (at 650 °C for 2 and 5 min) $GaAs_{0.949}N_{0.051}$ layers.

(i) the N out-diffusion [5] and (ii) the improvement of alloy uniformity resulting in the decrease of the value of the localization potential [14].

In order to qualitatively describe the evolution of the blue shifts, we have taken the (0 0 4) HRXRD $2\theta/\omega$ profiles, the (1 1 5) reciprocal space mapping, and the Raman spectra of the GaAsN layers before and after annealing. The changes in the N concentration resulting from annealing are concerned.

Fig. 3a shows the (0 0 4) HRXRD $2\theta/\omega$ curves of the GaAsN layers before and after annealing. The 2 min annealing resulted in a shift of the GaAsN diffraction peak to a higher angle, indicating an increasing of the N content. On the other hand, longer annealing time up to 5 min resulted in a shift of the GaAsN diffraction peak to a lower angle closer to the substrate peak. This may be resulting from a reduction of the N content. In contrast, the results of the (1 1 5) reciprocal space mapping of the 2 min (Fig. 3b) and 5 min (Fig. 3c) annealed samples indicate that the residual strain in all the annealed layers is partially relaxed. A reduction of the residual strain is due to the strain relaxation of the lattice by an introduction of misfit dislocations. Since, the rotation of the elliptic contours, which indicates the layer bending due to the

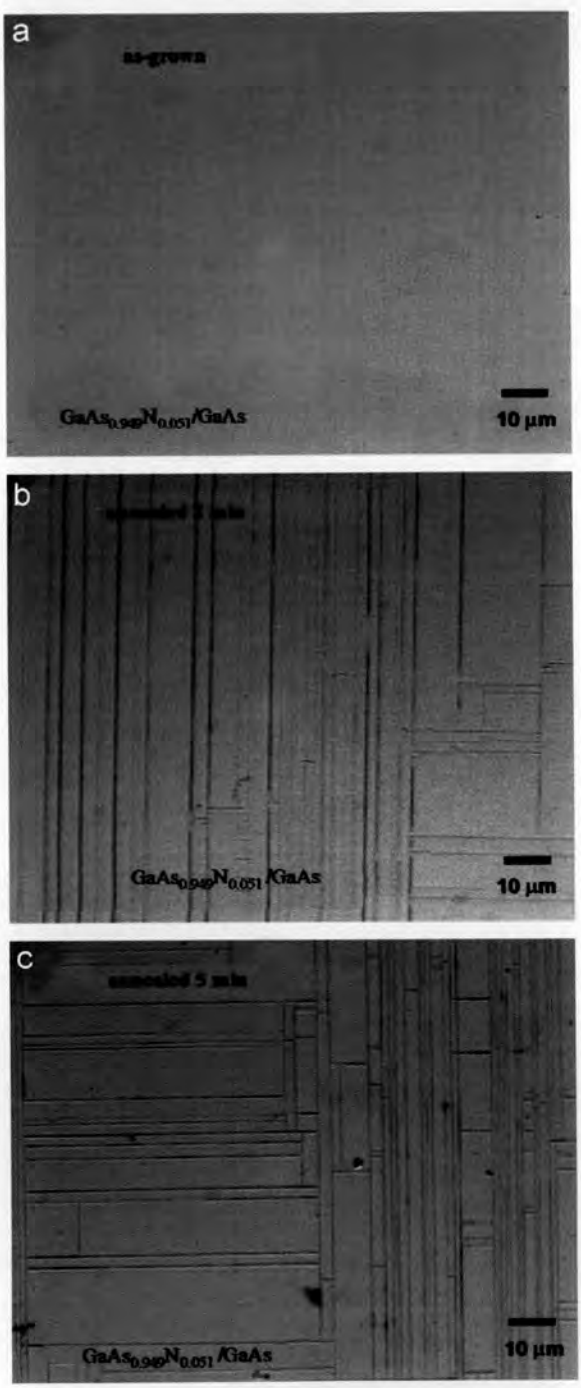

Fig. 5. Optical microscope images of the (a) as-grown and (b, c) annealed (at 650 °C for 2 and 5 min) $GaAs_{0.949}N_{0.051}$ layers.

residual strain, was reduced for longer annealing times. The shape of these diffraction points is considered to be broad along ω. These results demonstrate an influence of the post-growth thermal annealing is an increase of the tensile strain, which will produce the strain relaxation in such high N-containing layer, to a critical point of structural qualities of the layer.

It is also clearly seen in Fig. 4 that the normalized N-related local-vibrational mode (LVM) Raman intensity somewhat increases with an increasing of annealing time. Since, the integrated intensity of a Raman line is proportional to the number of corresponding oscillators [13]. Therefore, the integrated intensity of the N-related LVM in GaAsN is proportional to the N concentration in the layer. In addition, a gradual blue shift of the N-related LVM Raman frequency is also observed. This demonstrates an increase in the N content for longer annealing times. Hence, longer annealing up to 5 min did not result in the N out-diffusion. But, it may be well-justified that the strain relaxation has occurred in the annealed layers, as judged from surface cross-hatch patterns (Fig. 5) and resulting the disappearance of the Pendellösung fringes (Fig. 3a). These observations are consistent with the (0 0 4) HRXRD $2\theta/\omega$ scan and the (1 1 5) reciprocal space mapping results. Furthermore, the FWHM of the N-related LVM peak is gradually reduced when the annealing time is increased. This result is examined as a consequence of annealing-induced N diffusion inside the GaAsN material, which homogenizes initial N composition fluctuation.

HRXRD (Fig. 3) and Raman scattering (Fig. 4) results demonstrated that the thermal annealing could induce the blue shift of the PL spectra without necessarily a reduction of the N content. They therefore suggested that the interstitial N atoms generated in the growth process may substitute the As atoms/vacancies on the lattice sites to become more stable substitutional N atoms through the thermal annealing process, which will produce the strain relaxation in such high N-containing GaAsN layer. Furthermore, the diffusion of N atoms inside the layer homogenizes the initial N composition fluctuation in the as-grown alloy [14]. Note that no any indication of N out-diffusion was observable. Therefore, our results suggest that the two effects will account for the observed blue shift in the PL peak energy after annealing: (i) the improvement of alloy uniformity and (ii) the strain relaxation in such high N-containing $GaAs_{0.949}N_{0.051}$ layer.

4. Conclusions

Effect of post-growth thermal annealing on structural and optical properties of the high N-content $GaAs_{0.949}N_{0.051}$ layer was investigated. The dependence of N incorporation on the annealing time was studied by HRXRD and Raman scattering measurements. After annealing, an improvement of PL properties was clearly observed. PL spectrum with a near band edge exitonic emission without any deep-level-related luminescence and low-energy tail was obtained. With the longer annealing times, the PL peak energy showed a substantial blue shift, along with the long wavelength emission at about 1.3 μm (0.95 eV) was realized. The results of HRXRD and Raman scattering measurements demonstrate that in such high N-containing layer, the blue shift of PL spectra can be attributed to (i) the improvement of alloy uniformity and (ii) the strain relaxation.

Acknowledgments

The authors acknowledge S. Kuboya and K. Itagaki for their helpful cooperation in the MOVPE growth. Sincere thanks are extended to M. Tirarattanasompot, Scientific and Technology Research Equipment Centre (STREC) of Chulalongkorn University, for his technical support in X-ray diffraction measurements. This work has been supported by Thailand Research Fund (contact number MRG4880018), Thailand–Japan Technology Transfer Project–Overseas Economic Cooperation Fund (TJTTP–OECF), and Graduate School, Department of Physics, Faculty of Science, Chulalongkorn University.

References

[1] M. Kondow, T. Kitatani, S. Nakatsuka, M.C. Larson, K. Nakahara, Y. Yazawa, M. Okai, IEEE J. Select. Top. Quant. Electron. 3 (1997) 719.
[2] G. Mussler, L. Daweritz, K.H. Ploog, J. Crystal Growth 251 (2003) 399.
[3] I. Suemune, K. Uesugi, W. Walukiewicz, Appl. Phys. Lett. 77 (2000) 3021.
[4] J. Toivonen, T. Hakkarainen, M. Sopanen, H. Lipsanen, J. Crystal Growth 221 (2000) 456.
[5] L.H. Li, Z. Pan, W. Zhang, Y.W. Lin, Z.Q. Zhou, R.H. Wu, J. Appl. Phys 87 (2000) 245.
[6] M. Takahashi, A. Moto, S. Tanaka, T. Tanabe, S. Takagishi, K. Karatani, M. Nakayama, K. Matsuda, T. Saiki, J. Crystal Growth 221 (2000) 461.
[7] K. Uesugi, N. Morooka, I. Suemune, Appl. Phys. Lett. 74 (1999) 1254.
[8] H. Riechert, A. Yu Egorov, D. Livishits, B. Borchert, S. Illek, Nanotechnology 11 (2000) 201.
[9] D.E. Mars, D.I. Babic, Y. Kaneko, Y.-L. Chang, J. Vac. Sci. Technol. B 17 (3) (1999) 1272.
[10] F. Bousbih, S.B. Bouzid, A. Hamdouni, R. Chtourou, J.C. Harmand, Mater. Sci. Eng. B 123 (2005) 211.
[11] F. Nakajima, S. Sanorpim, W. Ono, R. Katayama, K. Onabe, Phys. Stat. Sol. (a) 203 (7) (2006) 1641.
[12] A. Kuzmin, N. Mironova, J. Phys.: Condensed Matter 10 (1998) 7937.
[13] M.J. Seong, M.C. Hanna, A. Mascarenhas, Appl. Phys. Lett. 79 (24) (2001) 3974.
[14] L. Grenouillet, C. Bru-Chevallier, G. Guillot, P. Ballet, P. Duvaut, G. Rolland, A. Million, J. Appl. Phys. 91 (2002) 5902.

APPENDIX B

PROCEEDING

Proceedings of the 2nd IEEE International
Conference on Nano/Micro Engineered and Molecular Systems
January 16 - 19, 2007, Bangkok, Thailand

Characterization of MOVPE Grown $GaAs_{1-x}N_x$/GaAs Multiple Quantum Wells Emitting Around 1.3-μm-Wavelength Region

P. Klangtakai[1], S. Sanorpim[1,*], K. Yoodee[1], W. Ono[2], F. Nakajima[2], R. Katayama[2], and K. Onabe[2]

[1]*Department of Physics, Faculty of Science, Chulalongkorn University, Phayathai Rd., Pathumwan, Bangkok 10330, Thailand.*

[2]*Department of Advanced Materials Science, TheUniversity of Tokyo, 5-1-5 Kashiwanoha, Kashiwa, Chiba, 277-8561, Japan.*

***Abstract*— $GaAs_{0.949}N_{0.051}$/GaAs multiple quantum wells (MQWs) were grown on GaAs (001) substrates by metalorganic vapor phase epitaxy (MOVPE). Strong photoluminescence (PL) emission around the 1.3-μm-wavelength region was observed without post-growth thermal annealing, which suggests an efficient electron confinement in the $GaAs_{0.949}N_{0.051}$/GaAs MQWs. After post-growth thermal annealing, blue-shift of PL peak energy was clearly observed. This PL blue-shift, induced by thermal annealing, can be described by diffusion of N out of the quantum well and homogenization of the N concentration fluctuation. Furthermore, a reduction of PL full width at half maximum (FWHM) suggests the more homogeneous N distribution. In addition, both the as-grown and annealed $GaAs_{0.949}N_{0.051}$/GaAs MQWs exhibit fairly flat and abrupt GaAsN/GaAs interfaces, which were confirmed by high resolution x-ray diffraction (HRXRD) and transmission electron microscopy (TEM) measurements. Based on PL results, it is evident that the band alignment of GaAsN/GaAs hetero-structure is a type-I band lineup. Adding N to GaAs mainly affects the conduction band (CB) states leading to a large conduction band offset (ΔE_C ~ 550 meV). Our results show the potential for the fabrication of 1.3 μm GaAsN QW lasers on GaAs substrates.**

Keywords-Multiple Quantum Wells; III-V-Nitrides; GaAs; Photoluminescence; high resolution x-ray diffraction; Laser diodes

I. INTRODUCTION

Nitrogen-containing III-V alloys have been studied intensively in recent years due to the large band gap bowing caused by the incorporation of a small amount of nitrogen [1]-[3]. Unlike the conventional ternary III-V semiconductor alloys, such as AlGaAs, GaInAs, GaInP, etc., where the band gap energy of the alloys can be approximated as a weighted linearly average of the band gaps of the parental binary compounds [4], [5]. The $In_yGa_{1-y}As_{1-x}N_x$ alloy material theoretically allows a large extension of emission wavelength, and an increased conduction band offset (ΔE_C) should lead to excellent laser operation at high temperature. The low-bandgap $In_yGa_{1-y}As_{1-x}N_x$-based quantum well (QW) structures are expected as useful for optoelectronic devices such as laser diodes (LDs) emitting at 1.3 and 1.55 μm for optical communication systems [6], [7]. The $GaAs_{1-x}N_x$ alloys with N concentrations (x) up to x ~ 0.05-0.08 were grown on a GaAs (001) substrate by metalorganic vapor phase epitaxy (MOVPE) [8], [9]. However, the optical quality of GaAsN alloy has been found to degrade with higher N incorporation. This may be due to the formation of highly inhomogeneous material with inclusions of GaN, GaAsN and GaAs phases [10]. This is because of an extremely large miscibility gap between GaN and GaAs caused by the large differences in lattice constant. Generally, post-growth thermal annealing is carried out to improve the luminescence properties, but leads to a blue-shift of the photoluminescence (PL) peak energy [11]. In addition, the improvement of optical quality by the GaAsN/GaAs QW structure is also concerned.

In this study, $GaAs_{0.949}N_{0.051}$/GaAs multiple quantum wells (MQWs) structures were grown by MOVPE. We report on PL experiments of the $GaAs_{0.949}N_{0.051}$/GaAs MQWs that reveal its origin at low-temperature. Discussion of the excitonic transition in the quantum wells is also given after presenting the results in more details, including well dimension and N concentration in the $GaAs_{1-x}N_x$/GaAs MQWs. In addition, the effect of post-growth thermal annealing was qualitatively investigated. PL emission wavelength as long as 1.3 μm at low-temperature (10K) was successfully achieved for both the as-grown and annealed $GaAs_{0.949}N_{0.051}$/GaAs MQWs.

II. EXPERIMENTS

$GaAs_{0.949}N_{0.051}$ bulk layer and $GaAs_{0.949}N_{0.051}$/GaAs multiple quantum wells (MQWs) structures were grown by MOVPE using trimetylgallium (TMGa), tertiarybutylarsine (TBAs) and 1, 1-dimethylhydrazine (DMHy) as the source materials for Ga, As and N, respectively. The $GaAs_{0.949}N_{0.051}$/GaAs MQWs consisted of 10-period GaAsN well and GaAs barrier layers. Sample structure of the $GaAs_{0.949}N_{0.051}$/GaAs MQWs is shown in Fig. 1. Thicknesses of the well and barrier layers were examined to be 5 and 26-27 nm, respectively. The N concentration in the GaAsN well layer and the well dimension were determined by HRXRD measurement via the dynamical-theory simulation software. Interface and micro-structural information were investigated by transmission electron microscopy (TEM). Optical properties of $GaAs_{0.949}N_{0.051}$/GaAs MQWs were examined by low-temperature (10 K) PL measurements. The 488 nm line of an Ar^+ laser is used as an excitation light source for the PL measurement. The luminescence was dispersed by a 0.3 m

This work was supported in part by Thailand Research Fund (Contact Number MRG4880018), Thailand-Japan Technology Transfer Project-Overseas Economic Cooperation Fund (TJTTP-OECF) and department of Physics, graduate school, Chulalongorn University.

* *Contact author: for fabrication aspects of this project please contact* ***Sakuntam.S@chula.ac.th.***

1-4244-0610-2/07/$20.00 ©2007 IEEE

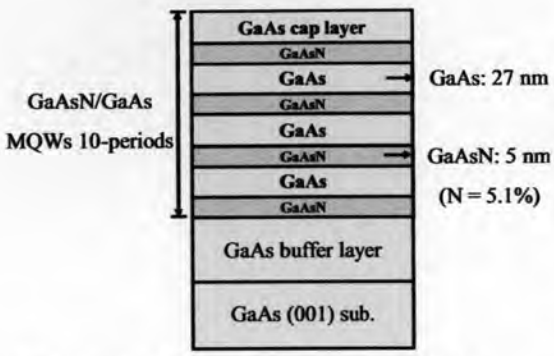

Fig. 1. Schematic diagram of the GaAsN/GaAs 10-period MQWs.

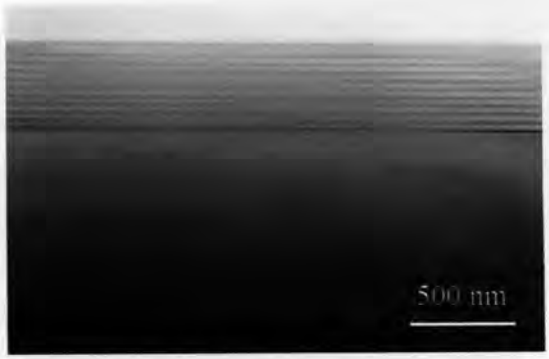

Fig. 2 Cross-sectional TEM image of as-grown $GaAs_{0.949}N_{0.051}$/GaAs 10-period MQWs.

monochromator, and detected by InGaAs p-i-n photodetector using the conventional lock-in technique. To improve the luminescence properties of $GaAs_{0.949}N_{0.051}$/GaAs bulk layer and MQWs, post growth thermal annealing in the growth reactor were performed at 650°C for 2 min under TBAs and H_2 ambient [12].

III. Results and Disscusion

A. *Determination of well dimension and N concentration*

Fig. 2 presents a cross-sectional bright field TEM image of as-grown $GaAs_{0.949}N_{0.051}$/GaAs MQWs. The TEM image reveals the sharp and well-defined interfaces between the GaAsN wells and the GaAs barriers. Thicknesses of the well and barrier layers obtained from the TEM image were estimated to be about 5 and 27 nm, respectively. Fig. 3 (a) illustrates a (004) HRXRD pattern obtained from the as-grown $GaAs_{0.949}N_{0.051}$/GaAs MQWs. As can be seen in Fig. 3 (a), the satellite peaks and Pendellösung fringes are clearly visible due to a finite thickness and high crystalline quality of the as-grown $GaAs_{0.949}N_{0.051}$/GaAs MQWs in spite of the high tensile strain in the QWs ($\Delta a/a = -1.02\times10^{-2}$). The separation between the nearest neighbor's satellite peaks is quite constant, showing that flat hetero-interfaces and uniform well-thickness are achieved. Also shown in the Fig. 3 is the dynamical-theory simulation result, curve (b), corresponding to curve (a). The fitted N concentration (x) inside the as-grown GaAsN well layer was $x = 0.051$. Thickness of the GaAsN well and GaAs barrier layers were estimated to be 5 nm and 26 nm, respectively. The period of GaAsN/GaAs stack becomes 31 nm, which is well comparable to the values determined from the cross-sectional TEM image. Based on TEM and HRXRD results, it is evident that a high epitaxial quality and coherently strained $GaAs_{1-x}N_x$/GaAs MQWs with N concentration as high as $x = 0.051$ was successfully grown by MOVPE.

B. *Optical characterization*

Low-temperature (10 K) PL results of the as-grown $GaAs_{0.949}N_{0.051}$/GaAs MQWs and a reference $GaAs_{0.949}N_{0.051}$ bulk layer, which was annealed at 650°C for 2 min, are shown in Fig. 4. Note that the PL emission from the as-grown bulk layer can not be detected because of the highly non-radiative recombination centers in such high N-containing layer. After post-growth thermal annealing, a single PL peak emission was clearly observed at 0.96 eV, which corresponds to the long wavelength emission at about 1.3 μm. This indicates that the annealing process can improve optical quality of such high N-containing GaAsN bulk layer. On the other hand, strong PL emission obtained from as-grown MQWs was observed. This reveals that the optical quality can be also improved by QW structures. Comparison with the annealed bulk layer, the PL peak energy of the as-grown MQWs blue-shift amounts to 80 meV. This large PL blue-shift is believed to be predominantly determined by the strong quantum confinement effect to the well. The PL emission from the as-grown MQWs was observed at about 1.04 eV. The difference between the PL peak position (1.04 eV) and high energy cut-off (1.10 eV) for as-grown MQWs is estimated to be 60 meV, this value is approximated to be a localization energy in the as-grown MQWs [13]. The PL emission from the as-grown MQWs has a board spectrum in the low energy region centered at 0.85 eV. In addition, faraway PL peaks at 1.451 and 1.506 eV are related to carbon-accepter and free exciton states of the GaAs, respectively. The difference between the PL peak positions of the bulk layer (0.96 eV) and the GaAs barrier (1.506 eV) is about 550 meV, indicating a large conduction band offset ($\Delta E_C \sim 550$ meV). This result demonstrates an efficient carrier confinement, which is realized in the high N-containing $GaAs_{1-x}N_x$/GaAs MQWs, giving higher efficient PL emission at higher temperatures. To understand the origin of PL obtained from the $GaAs_{1-x}N_x$/GaAs MQWs, so the band alignment in this hetero-structure system is concerned.

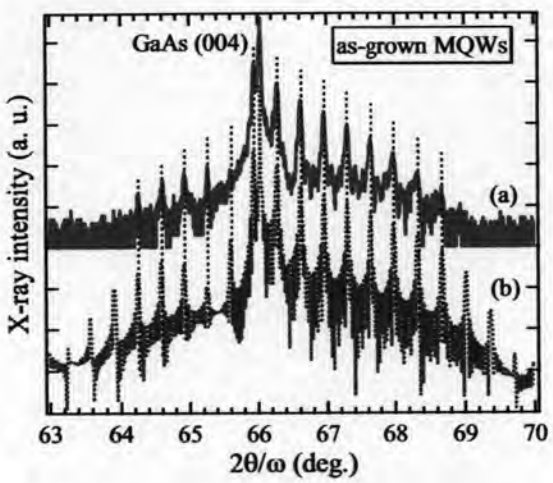

Fig. 3. (004) XRD patterns of as-grown $GaAs_{0.949}N_{0.051}$/ GaAs 10-period MQWs. The (a) solid curve is the experimental data and (b) the dashed curve is a simulated result using the dynamic theory.

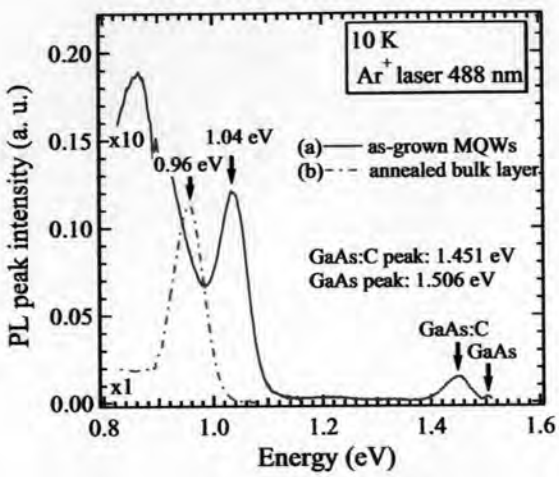

Fig. 4. Low-temperature (10K) PL spectra of (a) as-grown $GaAs_{0.95}N_{0.05}$/GaAs MQWs and (b) reference $GaAs_{0.949}N_{0.051}$ bulk layer, which was annealed at 650°C for 2 min.

C. *Band alignment of GaAsN/GaAs hetero-structure*

1) Bandgap calculation

One of the remaining unsolved issues regarding the electronic properties of the GaAsN/GaAs QWs structure involves the band alignment. Here we discuss on the fundamental types of the band alignment of the GaAsN/GaAs QWs structure. Fig. 5 shows promising types of band alignment of the GaAsN/GaAs QWs, namely (a) a type-I and (b) a type-II QWs structures. To establish the band alignment, the bandgap energy of GaAsN is determined using the band anticrossing (BAC) model, which was proposed by Shan *et al.* [14]. This model describes an interaction between the highly localized N state and conduction band state and also used to explain the bandgap behavior, including pressure and temperature dependences, for the dilute III-V-nitride system. Addition of N concentration (x) contributes to the bandgap change according to

$$E_g(x) = \frac{E_M + E_N \pm \sqrt{[E_M - E_N]^2 + 4V_{MN}^2 \cdot x}}{2}. \quad (1)$$

Where x denotes the N concentration and $E_g(x)$ is the bandgap energy of corresponding $GaAs_{1-x}N_x$ alloy. Where the top of valence band is taken as a reference energy level, E_M is the extended conduction band of GaAs, E_N is an impurity level due to N incorporation assumed here to be located at 1.65 eV above the valence band of GaAs [15]. V_{MN} is the coupling between the extended conduction band state (E_M) and the nitrogen state (E_N). The V_{MN} parameter is a fitting parameter, for GaAsN alloy system V_{MN} = 2.7 eV [15]. Along with (1), bandgap of $GaAs_{0.949}N_{0.051}$ alloy at 300 K is calculated to be 0.917 eV. However, our PL results shown in Fig. 4 were obtained at low-temperature of 10 K. Then, the empirical Varshni's model [16] was used to determine the bandgap of $GaAs_{0.949}N_{0.051}$ alloy at 10 K. By varying the temperature T, the bandgap is

$$E_g(T) = E_g(0) - \frac{\alpha T^2}{\beta + T}. \quad (2)$$

Where E_g(T) and E_g(0) are the bandgap of $GaAs_{1-x}N_x$ at temperatures T and absolute zero, respectively. The values of α and β for $GaAs_{1-x}N_x$ alloy system is expected to obey Vergard's law, i. e., to very linear with the N concentration (x). For $GaAs_{0.949}N_{0.051}$ alloy, the values of α and β can be determined using a linear interpolation between these values of GaAs and zinc-blend GaN. The values of α and β for GaAs and zinc-blend GaN are summarized in Table I. The determined values of α and β for $GaAs_{0.949}N_{0.051}$ also listed in Table I. According to (2), $E_g(0)$ of $GaAs_{0.949}N_{0.051}$ is calculated to be 1.012 eV. Thus, the bandgap of $GaAs_{0.949}N_{0.051}$ at 10 K (E_g(10K)) is estimated to be 1.011 eV.

In order to calculate ΔE_C of $GaAs_{1-x}N_x$/GaAs QWs structure, the valence band offset (ΔE_V) is a required consideration. Sakai *et al.* theoretically predicted that bowing of the valence band of the dilute $GaAs_{1-x}N_x$ alloy is negligible [19]. Thus, in the present study, the natural valence band (E_V) alignment of the $GaAs_{1-x}N_x$ alloy was approximately evaluated using a linear interpolation between the values of E_V of GaAs and zinc-blend GaN (see in Table I). The value of ΔE_V of $GaAs_{1-x}N_x$/GaAs QWs structure is calculated by setting the E_V alignment of GaAs as a reference energy level. Therefore, the value of ΔE_V of the $GaAs_{1-x}N_x$/GaAs QWs system can be expressed as

$$\Delta E_v(x) = -2.18 \cdot x. \quad (3)$$

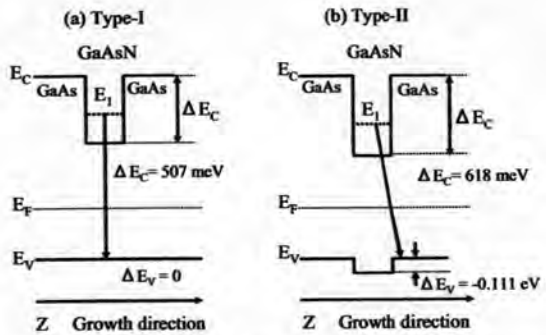

Fig. 5. Schematic band diagrams of the quantum structures with (a) the type-I and type-II band alignment and their expected properties.

Along with (3), we found that $GaAs_{1-x}N_x$/GaAs heterostructure have a negative valence band offset. The value of ΔE_V is estimated to be - 0.111 eV for the $GaAs_{0.949}N_{0.051}$/GaAs QWs structure. Therefore, the fundamental type of the band alignment of the $GaAs_{1-x}N_x$/GaAs QWs structure is should be type-II band lineup, as shown in Fig. 5(b). However, in the present case, the value of ΔE_C for $GaAs_{0.949}N_{0.051}$/GaAs QWs structure is approximately determined to be ~ 618 meV, which is much larger than the estimated value of ΔE_C (~ 550 meV) from the difference between the PL peak positions of the annealed $GaAs_{0.949}N_{0.051}$ bulk layer and the GaAs barrier, as shown in Fig. 4. In addition, based on HRXRD results, the N concentration inside the $GaAs_{0.949}N_{0.051}$ bulk layer is increased with post-growth thermal annealing treatment [21]. As a result, we expect that the value of ΔE_C for $GaAs_{0.949}N_{0.051}$/GaAs QWs should be smaller than 550 meV at 10 K. These results strongly suggest that the type-II band lineup may be unable to explain the optical transition in the $GaAs_{1-x}N_x$/GaAs QWs. In order to continue understanding the band alignment of $GaAs_{1-x}N_x$/GaAs QWs structure, therefore, the excitonic transition energy inside the well layer is mentioned.

2) Excitonic transition energy

The recombination process inside the well layer is originated from the excitonic recombination. For the tensile strained GaAsN/GaAs QWs, thus inside the well layer, the light hole state exhibits higher than the heavy hole state. As a consequence, the effective mass inside the well can be determined by reduced mass between the electron effective mass (m^*_e) and light hole effective mass (m^*_{lh}), which are evaluated at the Brillouin zone center. The value of m^*_e, which is estimated from BAC model [14], is given by

$$m_e^* \approx \hbar^2 \left| \frac{k}{dE_-(k)/dk} \right|_{k=0} = 2m_{e,GaAs}^* \Big/ \left[1 - \frac{E_M - E_N}{\sqrt{(E_M - E_N)^2 + 4V^2 x}} \right]. \quad (4)$$

Using (4), the value of m^*_e for the $GaAs_{0.949}N_{0.051}$ alloy was calculated to be $0.1133m_0$. On the other hand, the value of m^*_{lh} for $GaAs_{1-x}N_x$ can be approximately determined using a linear interpolation between the values of m^*_{lh} of GaAs and zinc-blend GaN. The lists of m^*_e and m^*_{lh} for GaAs and zinc-blend GaN are summarized in Table I. For $GaAs_{0.949}N_{0.051}$ alloy, the value of m^*_{lh} is determined to be $0.049m_0$.

In case of the $GaAs_{0.949}N_{0.051}$/GaAs type-II band lineup, the ΔE_V and ΔE_C are estimated to be -0.111 eV and 618 meV. We applied the finite-depth single-square well model to calculate the confinement energies inside the well layer. The transition energy is approximated to be the critical transition from the GaAs valence band edge to the ground state in the confined energies (see Fig. 5(b)). At low-temperature of 10 K, the transition energy for the $GaAs_{0.949}N_{0.051}$/GaAs QWs type-II band lineup with well width of 5 nm is calculated to be 1.042 eV. Comparison with the PL peak position obtained from the as-grown $GaAs_{0.949}N_{0.051}$/GaAs MQW (1.04 eV), as show in Fig. 4(a), the calculated transition energy is comparable to the PL peak energy. On the other hand, temperature dependent PL measurements of the as-grown $GaAs_{0.949}N_{0.051}$/GaAs MQWs (not shown) demonstrate that the PL emission is attributed the localized exciton states. The localization energy for the as-grown $GaAs_{0.949}N_{0.051}$/GaAs MQWs was determined to be about 100 meV at 10 K. This means that the value of the transition energy should be larger than 1.042 eV at 10 K. As a consequence, it is established that the optical transition of the $GaAs_{1-x}N_x$/GaAs QWs structure can not be explained by the type-II band lineup.

Another way, we discuss on the $GaAs_{1-x}N_x$/GaAs type-I band lineup. Schematic band diagram of the type-I band lineup is shown in Fig. 5(a). It is known that adding N into GaAs decreases the bandgap, which mainly affects the conduction band (CB) states leading to a large ΔE_C and only a small valence band (VB) discontinuity [24]. Thus, the value of ΔE_V can be approximated to be zero, in our case. Accordingly, the value of ΔE_C for the $GaAs_{0.949}N_{0.051}$/GaAs QWs structure, which determined from the difference of E_g (10 K) between GaAs and $GaAs_{0.949}N_{0.051}$/GaAs, is 507 meV. Then, the calculated transition energy at 10 K for the $GaAs_{0.949}N_{0.051}$/GaAs MQWs with well width of 5 nm is 1.145 eV. It is showed that the difference between calculated transition energy (1.145 eV) and the PL peak position (1.04 eV) of as-grown $GaAs_{0.949}N_{0.051}$/GaAs MQWs is estimated to be 105 meV. This value is comparable with the localization

TABLE I
BAND STRUCTURE PARAMETERS

Symbol	GaAs	zinc-blend GaN	$GaAs_{0.949}N_{0.051}$
α ($\times 10^{-4}$ eV/K)	5.405 [17]	7.7 [18]	5.522
β (K)	204 [17]	600 [18]	224
E_g(0 K) (eV)	1.519 [17]	3.28 [18]	1.012
E_g(10K) (eV)	1.518	3.27	1.011
E_g(300K) (eV)	1.424 [17]	3.2 [18]	0.917
E_V (eV)	1.46 [20]	-0.72 [20]	1.35
m^*_e	$0.067m_0$ [17]	$0.15m_0$ [18]	$0.1133m_0$
m^*_{lh}	$0.082m_0$ [22]	$0.19m_0$ [23]	$0.049m_0$

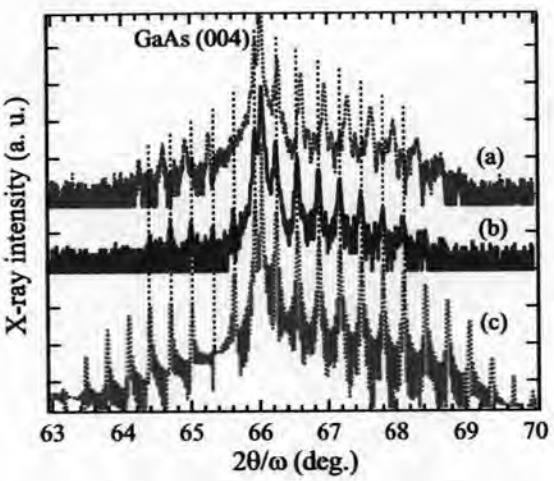

Fig. 6. (004) XRD patterns of (a) as-grown, (b) annealed 10-period $GaAs_{0.949}N_{0.051}$/GaAs MQWs are the experimental data, and (c) the dashed curve is a simulation result using the dynamic theory for annealed MQWs.

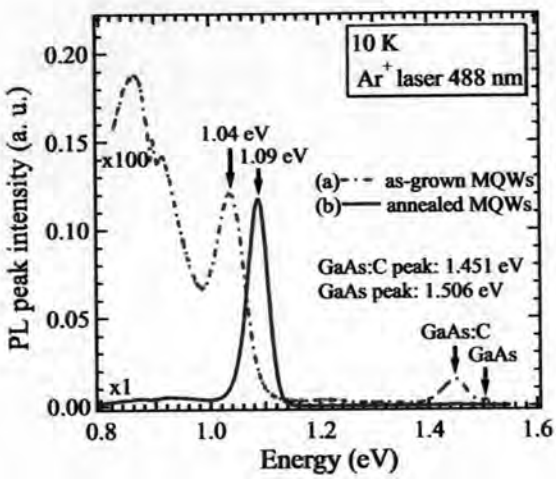

Fig. 7. Low-temperature (10K) PL spectra of the (a) as-grown and (b) the annealed $GaAs_{0.949}N_{0.051}$/GaAs MQWs.

energy of the as-grown MQWs, which is investigated from temperature dependent PL measurements. The results imply that the calculated transition energy for the type-I band lineup is well consistent with the experimental results. Finally, we suggest that the type-I band lineup is a suitable band alignment, describing the optical transition in the $GaAs_{1-x}N_x$/GaAs QWs structure.

D. Annealing Effects on Optical Property

Fig. 6 shows (004) HRXRD patterns, which obtained from (a) as-grown, (b) annealed (650°C, 2 min) $GaAs_{0.949}N_{0.051}$/GaAs MQWs, and (c) simulation result using the dynamical-theory for annealed MQWs. The satellite peaks and Pendellösung fringes are still clearly visible for the annealed MQWs, as shown in Fig. 6 (b). These results indicate that the high N-containing as-grown and annealed MQWs are coherently strained without any indication of strain relaxation. In Fig. 6 (b), thermal annealing resulted in a shift of the satellite peaks to a lower diffraction angle, indicating a reduction of the N concentration in the well, which is verified by the dynamical-theory simulation results. The fitted N concentration (x) inside the annealed GaAsN well layer was x = 0.048. Furthermore, it is also found that the separation between the nearest neighbor's interference fringes is quite the same as the as-grown sample. This suggests that there is no change in the thicknesses of the well layer. According to almost fitting results, the thickness of the well layer was also determined to be 5 nm.

Low-temperature (10 K) PL spectra of the (a) as-grown and (b) annealed $GaAs_{0.949}N_{0.051}$/GaAs MQWs, are shown in Fig. 7. After annealing, the peak intensity of the quantum well emission is increased by a factor of 100, indicating the improvement of optical quality induced by the reduction of non-radiative recombination centers is clearly observed. The PL peak position shows a blue-shift of approximately 50 meV from 1.04 to 1.09 eV. In general, this blue shift of PL peak position suggest that the annealing induces (i) diffusion of N out the well layers, (ii) strain relaxation in the GaAsN well layer, and (iii) homogenizes the localization potential due to the N distribution fluctuations. Based on the HRXRD results, in the present case, the blue shift of PL peak position indicates that the annealing induces diffusion of N out the well layers and homogenizes the localization potential due to the N distribution fluctuations. No strain relaxation in the GaAsN well layers was observed. It is also evidence that, after annealing, PL full width at half maximum (FWHM) is decreased from 72 to 43 meV, confirming the improvement of composition uniformity.

Fig. 8 illustrates the calculated transition energy of $GaAs_{1-x}N_x$/GaAs (x = 0.048 and 0.051) MQWs type-I band lineup, which has been calculated by finite-depth single-square well model. The transition energy is attributed to the critical transition from the valence band edge to the ground state in the confined energies. The transition energy at 10 K for annealed $GaAs_{0.952}N_{0.048}$/GaAs type-I band lineup is estimated to be 1.161 eV, as indicate by dashed line. The difference between the calculated transition energy (1.161 eV) and the PL peak position (1.09 eV) for the annealed $GaAs_{0.952}N_{0.048}$/GaAs MQWs at 10 K is about 71 meV, which is comparable to the localization energy obtained by the temperature dependent PL measurements (~ 60 meV) (not shown). This suggests that the annealing homogenizes the N distribution in the well layers, resulting in the reduction of localization energy. Also, the difference between the PL peak position (1.09 eV) and high energy cut-off (1.14 eV) for the annealed MQWs was estimated to be 50 meV. This value is smaller than that in as-grown MQWs, indicating that the

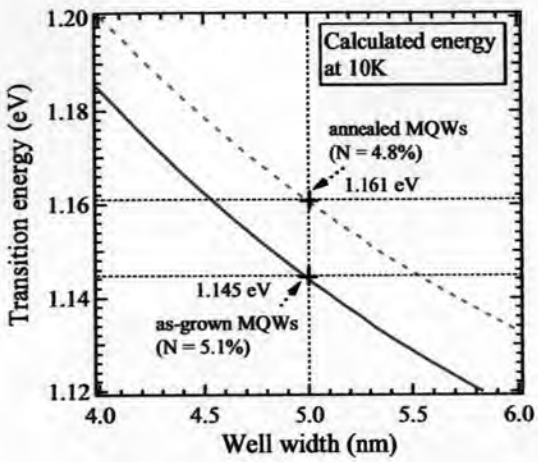

Fig. 8. Calculated transition energy at low-temperature (10K) of GaAsN/GaAs MQWs type-I band lineup as a function of N concentration (x) and well width. The solid line and dashed line are the calculated transition energy for $GaAs_{0.949}N_{0.051}$/GaAs and $GaAs_{0.952}N_{0.048}$/GaAs MQWS, respectively.

localization energy is decreased after post-growth thermal annealing. This confirms that the composition uniformity can be improved by annealing process.

IV. Conclusion

Optical and structural properties of the high-N content $GaAs_{0.949}N_{0.051}$/GaAs MQWs were investigated. The N concentration and well dimension were examined by HRXRD and TEM measurements. The PL spectra of the as-grown and annealed $GaAs_{0.949}N_{0.051}$/GaAs MQWs show a strong emission at around the 1.3 μm wavelength region. The calculated transition energy using the finite-depth single-square well **model showed the band alignment of $GaAs_{1-x}N_x$/GaAs hetero-**structure is a type-I band lineup. The large conduction band **offset ($\Delta E_C \sim 550$ meV) which indicates a large barrier height** for an electron confinement in the $GaAs_{0.949}N_{0.051}$/GaAs MQWs was established. After annealing, the PL peak energy showed a significant blue shift. Based on HRXRD and TEM results, in such high-N containing MQWs, the PL blue shift is attributed to the N out diffusion and the improvement of alloy uniformity. These results demonstrate that the possibility of fabricating GaAsN-based optoelectronic devices for optical-**fiber communications the wavelength region around 1.3 μm** can operate giving higher efficient PL emission at higher temperatures.

References

[1] A. J. Ptak, S. Kurtz, C. Curtis, R. Reedy and J. M. Olson, "Incorporation effects in MOCVD-grown (In)GaAsN using different nitrogen precursors," J. Crystal Growth, vol. 243, 2002, pp. 231-237.

[2] M. Kondow, K. Uomi, A. Niwa, T. Kitatani, S. Watahiki and Y. Yazawa, "GaInNAs: A Novel Material for Long-Wavelength-Range Laser Diodes with Excellent High-Temperature Performance," Jpn. J. Appl. Phys., vol. 35, 1996, pp. 1273-1275.

[3] M. Weyers, M. Sato and H. Ando, "Growth of GaAsN alloys by low-pressure metalorganic chemical vapor deposition using plasma-cracked NH_3," Appl. Phys. Lett., vol. 62, 1993, pp. 1396-1398.

[4] K. Uesugi and I. Suemune, "Bandgap Energy of GaNAs Alloys Grown on (001) GaAs by Metalorganic Molecular Beam Epitaxy," Jpn. J. Appl. Phys., vol. 36, 1997, pp. L1572-L1575.

[5] S. Sakai, Y. Ueta, Y. Terauchi, "Band Gap Energy and Band Lineup of III-V Alloy Semiconductors Incorporating Nitrogen and Boron," Jpn. J. Appl. Phys., vol. 32, 1993, pp. 4413-4417.

[6] G. Mussler, L. Daweritz and K. H. Ploog, "Thickness dependent roughening of Ga(As,N)/GaAs MQW structures with high nitrogen content," J. Crystal Growth, vol. 251, 2003, pp. 399-402.

[7] I. Suemune, K. Uesugi and W. Walukiewicz, "Role of nitrogen in the reduced temperature dependence of band-gap energy in GaNAs," Appl. Phys. Lett., vol. 77, 2000, pp. 3021-3023.

[8] J. Toivonen, T. Hakkarainen, M. Sopanen and H. Lipsanen, "High nitrogen composition GaAsN by atmospheric pressure metalorganic vapor-phase epitaxy," J. Crystal Growth, vol. 221, 2000, pp. 456-460.

[9] L. H. Li, Z. Pan, W. Zhang, Y. W. Lin, Z. Q. Zhou and R. H. Wu, "Effects of rapid thermal annealing on the optical properties of GaN_xAs_{1-x}/GaAs single quantum well structure grown by molecular beam epitaxy," J. Appl. Phys., vol. 87, 2000, pp. 245-248.

[10] C. T. Foxon, T. S. Cheng, S. V. Novikov, D. E. Lacklison, L. C. Jenkins, D. Johnston, J. W. Orton, S. E. Hooper, N. Baba-Ali, T. L. Tansley and V. V. Tret'yakov, "The growth and properties of group III nitrides," J. Crystal Growth, vol. 150, 1995, pp. 892-896.

[11] K. Uesugi, N. Morooka and I. Suemune, "Reexamination of N composition dependence of coherently grown GaNAs band gap energy with high-resolution X-ray diffraction mapping measurements," Appl. Phys. Lett., vol. 74, 1999, pp. 1254-256.

[12] F. Nakajima, S. Sanorpim, W. Ono, R. Katayama and K. Onabe, "MOVPE growth and optical characterization of GaAsN films with high nitrogen concentration," phys. Stat. sol. (a), vol. 203, 2006, pp. 1641-1644.

[13] C. Carballeira, J. Mosqueira, M. V. Ramallo, J. A. Veira and F. Vidal, "Fluctuation-induced diamagnetism in bulk isotropic superconductors at high reduced temperatures," J. Phys.: Condens. Matter, vol. 13 pp. 9271-9279.

[14] W. Shan, W. Walukiwicz, J. W. Ager III, E. E. Haler, J. F. Geisz, D. J. Friedman, J. M. Olson, S. R. Kurtz, "Band Anticrossing in GaInNAs Alloys," Phys. Rev. Lett., vol. 82, 1999, pp. 1221-1224.

[15] J. Wu, W. Shan and W. Walukiwicz, "Band anticrossing in highly mismatched III-V semiconductor alloys," Semicond. Sci. Technol., vol. 17, 2002, pp. 860-869.

[16] M.-A. Pinault and E. Tournie, "On the origin of carrier localization in $Ga_{1-x}In_xN_yAs_{1-y}$/GaAs quantum wells," Appl. Phys. Lett., vol. 78, 2001, pp. 1562-1564.

[17] J. S. Blakemore, "Photoelectric memory effect in GaAs," J. Appl. Phys. vol. 53, 1982, pp. 3643-3649.

[18] S. Sakai and T. Abe, "Band lineup of nitride-alloy heterostructures," in 41st Spring Meet. Jpn. Soc. Appl. Phys., Tokyo, Japan, 1994, pp. 186.

[19] V. Bougrov, M. E. Levinshtein, S. L. Rumyantsev, A. Zubrilov, "in Properties of Advanced SemiconductorMaterials GaN, AlN, InN, BN, SiC, SiGe," Eds. Levinshtein M.E., Rumyantsev S.L., Shur M.S., John Wiley & Sons, Inc., New York, 2001, 1-30.

[20] S.-H. Wei and A. Zunger, "Calculated natural band offsets of all II-VI and III-V semiconductors: Chemical trends and the role of cation d orbitals," Appl. Phys. Lett., vol. 72, 1998, pp. 2011-2013.

[21] P. Klangtakai, S. Sanorpim, K. Yoodee, W. Ono, F. Nakajima, R. Katayama and K. Onabe, "Post-growth thermal annealing of high-N content GaAsN by MOVPE and its effect on strain relaxation," J. Crystal Growth., in press.

[22] S. M. Sze, Physics of Semiconductor Devices, John Wiley & Sons, New York (1981).

[23] K. Kim, W. R. L. Lambrecht, B. Segall and M. van Schilfgaarde, "Effective masses and valence-band splittings in GaN and AlN," Phys. Rev. B, vol. 56, 1997, pp. 7363-7375.

[24] M. Kozhevnikov, V. Narayanamurti, C. V. Reddy, H. P. Xin, C. W. Tu, A. Mascarenhas and Y. Zhang, "Evolution of $GaAs_{1-x}N_x$ conduction states and giant Au/$GaAs_{1-x}N_x$ Schottky barrier reduction studied by ballistic electron emission spectroscopy," Phys. Rev. B, vol. 61, 2000, pp. R7861-R7864.

APPENDIX C

CONFERENCE PRESENTATIONS

1. **P. Klangtakai**, S. Sanorpim, K. Yoodee, W. Ono, F. Nakajima, R. Katayama and K. Onabe. Annealing effect on strain relaxation of high-N content GaAsN films. *14th Academic Conference*. Faculty of Science, Chulalongkorn University, Thailand, March 16-17, 2006 **(Oral presentation)**.

2. **P. Klangtakai**, S. Sanorpim, K. Yoodee, W. Ono, F. Nakajima, R. Katayama and K. Onabe. Post-growth thermal annealing of high-N content GaAsN by MOVPE and its effect on strain relaxation. *13th International Conference on Metal Organic Vapor Phase Epitaxy*. PHOENIX SEAGAIA RESORT, Miyazaki, Japan, May 22-26, 2006 **(Poster presentation)**.

3. **P. Klangtakai**, S. Sanorpim, K. Yoodee, W. Ono, F. Nakajima, R. Katayama and K. Onabe. Thermal annealing effect on optical properties of $GaAs_{1-x}N_x$/GaAs multiple quantum wells structure with high N content grown by MOVPE. *32nd Congress on Science and Technology of Thailand (STT.32)*. Thailand, October 10-12, 2006 **(Poster presentation)**.

4. **P. Klangtakai**, S. Sanorpim, K. Yoodee, W. Ono, F. Nakajima, R. Katayama and K. Onabe. Thermal annealing effect on strain relaxation of GaAsN films with high N content grown by MOVPE. *The 6th National Symposium on graduate Research*. Graduate School Chulalongkorn University, October 13-14, 2006 **(Oral presentation)**.

5. **P. Klangtakai**, S. Sanorpim, K. Yoodee, W. Ono, F. Nakajima, R. Katayama, and K. Onabe. Characterization of MOVPE grown $GaAs_{1-x}N_x$/GaAs multiple quantum wells emitting around 1.3-μm-wavelength region. *2nd IEEE International Conference on Nano/Micro Engineered and Molecular Systems*. Bangkok, Thailand, January 16-19, 2007 **(Poster presentation)**.

6. **P. Klangtakai**, S. Sanorpim, K. Yoodee, W. Ono, F. Nakajima, R. Katayama and K. Onabe. Investigation of $GaAs_{1-x}N_x$/GaAs type-I quantum wells. *Siam Physics Congress (SPC)*, March 22-24, 2007 **(Oral Presentation)**.

7. **P. Klangtakai**, S. Sanorpim, K. Yoodee, R. Katayama, and K. Onabe. Characteristics of GaAsN/GaAs type-I quantum wells grown by metalorganic vapor phase epitaxy on GaAs (001) substrates. *International Conference on Materials for Advanced Technologies 2007 (ICMAT)*. July 1-6, 2007 **(Accepted for Oral Presentation)**.

VITAE

Miss Pawinee Klangtakai was born on 9th April 1981 in Roi-Et, Thailand. She has been a student in the Development and Promotion for Science and Technology Talents Project (DPST). She received her Bachelor degree of Science in Physics from Khon Kaen University in 2003, and continued her Master's degree study at Chulalongkorn University in 2004.

She has published one international scientific paper in Journal of Crystal Growth, which have the impact factor of 1.68 (APPENDIX A). She has participated three international conferences, as follows:

1. 13th International Conference on Metal Organic Vapor Phase Epitaxy, May 22-26, Japan (APPENDIX A);

2. 2nd IEEE International Conference on Nano/Micro Engineered and Molecular Systems, January 16-19, Thailand (APPENDIX B) and

3. International Conference on Materials for Advanced Technologies 2007 (ICMAT), July 1-6, Singapore (APPENDIX C).

In addition, she also participated in local conference for four times (APPENDIX C).